Biochemistry

pubs.acs.org/biochemistry Article

Concerted Deoligomerization and Nonfunctional Reassembly of the Hexameric Proteasomal ATPase Mpa upon Chemical and Thermal Perturbation

Pushpkant Sahu, Samapti Mondal, Bincy Lukose, Thalappil Pradeep, and Hema Chandra Kotamarthi*

Cite This: https://doi.org/10.1021/acs.biochem.5c00642 Read Online

ACCESS | Metrics & More | Article Recommendations | Supporting Information

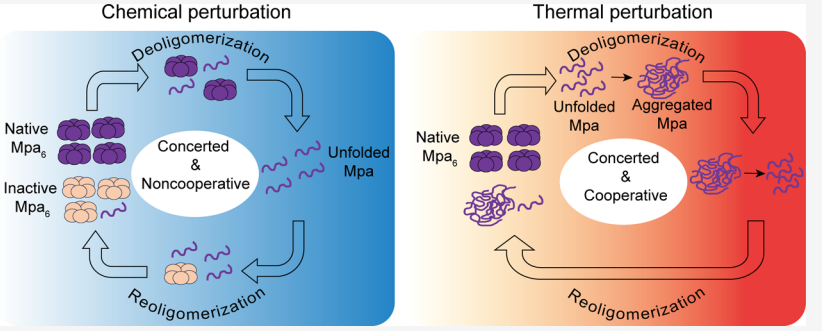

ABSTRACT: *Mycobacterium tuberculosis* Mpa is an AAA+ ATPase that unfolds and translocates substrate proteins during proteasomal degradation. Mpa spontaneously assembles into a homohexamer driven by interdomain interactions, even in the absence of a nucleotide. To dissect the mechanisms underlying its oligomerization and deoligomerization, we perturbed the system using chemical and thermal denaturants and monitored the oligomeric states by far-UV CD, fluorescence, calorimetry, state-of-the-art single-particle mass photometry, and ATPase activity assays. Equilibrium chemical denaturation resulted in gradual changes in spectroscopic signals, whereas mass photometry revealed a direct transition from a hexamer to monomeric species, indicating a concerted but noncooperative pathway without any intermediate oligomeric or folded monomeric states. In contrast, thermal perturbation showed two sharp and distinct transitions, the first one corresponding to a concerted and cooperative transition from hexamer to unfolded state, which further aggregates, and the second transition to disaggregation at elevated temperatures. Both chemical and thermal unfolding processes were irreversible with respect to the reassembly of the functional oligomer. Using single-particle mass photometry complemented by spectroscopy and calorimetry, these findings establish that Mpa is an obligate oligomer and can provide insights into the oligomerization pathways of AAA+ enzymes that spontaneously hexamerize and have the potential to further illuminate evolutionary strategies underlying their assembly mechanisms.

INTRODUCTION

Oligomerization is a common feature in proteins that contributes to functional specialization and enhanced structural stability. Homo-oligomeric proteins are prevalent across species and display considerable diversity in pathways during deoligomerization and reoligomerization.[1−5] Some of the hexameric homo-oligomeric chaperone and nonchaperone proteins, such as Hsp16.3 and RbsD, have been observed to follow a stepwise disassembly,[6,7] whereas chaperones such as GroEL have been shown to remain tetradecameric but undergo quaternary structure conformational changes before dissociation. The AAA+ (ATPases Associated with diverse cellular Activities) family represents a widespread class of oligomeric enzymes involved in critical cellular processes such as DNA replication, protein degradation, and membrane remodeling. A large number of these AAA+ enzymes assemble into closed-ring hexameric structures, and this oligomeric architecture is essential for ATP hydrolysis, which drives their mechanical function.[8−12] The ATPases involved in protein degradation, such as ClpX, ClpA, and PAN, typically form symmetric homohexamers that regulate substrate entry into the associated peptidase compartments.[13,14] Many of these ATPases form hexamers only in the presence of nucleotide and predominantly exist as monomers or dimers in the absence of a nucleotide. ClpA proceeds through monomer−dimer-tetramer assembly, whereas p97 hexamerizes even in the absence of nucleotide and deoligomerizes directly into a monomeric state

Received: October 17, 2025
Revised: January 23, 2026
Accepted: January 27, 2026

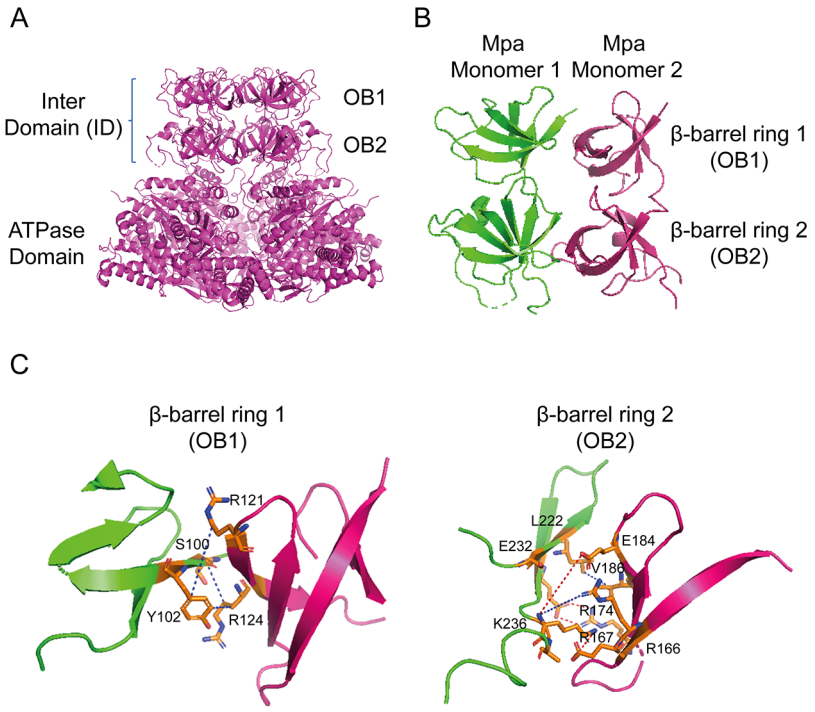

Figure 1. (A) X-ray crystal structure of the Mpa homohexamer (PDB ID: 5KZF), with ATPase domain and the interdomains (OB1 and OB2) highlighted. The coiled-coil domain is a flexible region and is not shown in the structure. (B) Individual OB domains (OB1 and OB2) from monomeric units in a Mpa hexamer. (C) Interactions between OB domains of adjacent Mpa monomers. Hydrophobic and electrostatic interactions are indicated by blue and red dashed lines, respectively.

upon urea denaturation and can reassemble into an active hexamer upon renaturation.[9,15−19]

The mycobacterial proteasomal ATPase, Mpa, from *Mycobacterium tuberculosis* (*Mtb*), is one such AAA+ enzyme that forms hexamers and facilitates the degradation of pupylated protein substrates. Like other proteasomal AAA+ ATPases, Mpa functions as a mechanoenzyme, unfolding and translocating substrates into the 20S core protease (20S CP) for degradation. Unlike many other AAA+ enzymes, Mpa spontaneously assembles into stable homohexamers even in the absence of nucleotides[20−23] (Figure S1). Mpa has four major domains: the ATPase domain, two oligosaccharide-binding (OB) domains together referred to as the interdomain (ID) (Figure 1A), and a flexible coiled-coil domain (not shown). Structural and mutational analyses have shown that hexamer stabilization primarily arises from interactions between the OB domains of individual monomers (Figure 1B). In particular, the OB2 domains play a dominant role, with stabilization contributed through a combination of electrostatic and hydrophobic interactions[23,24] (Figure 1C).

Despite extensive biochemical, structural, and functional studies, the mechanisms underlying the oligomerization, deoligomerization, and stability of hexameric AAA+ assemblies remain incompletely understood, particularly for the enzymes that hexamerize in an ATP-independent manner. It is unclear whether these enzymes assemble through defined intermediates (such as dimers or trimers) or transition directly from monomers to hexamers. Studying the deoligomerization/reoligomerization pathways of homo-oligomers can pave the way for a mechanistic understanding of their oligomerization pathways and has been used to understand the evolutionary pathways of protein complex formation.[1,25,26] The intrinsic ability of Mpa to form stable hexamers independent of nucleotides makes it a good model system to investigate the oligomerization pathways of AAA+ hexamers. In this study, we examined the urea-induced chemical and heat-induced thermal deoligomerization and reoligomerization mechanisms of Mpa. To characterize the structural, oligomeric, and functional states of Mpa under these perturbations, we employed a combination of spectroscopic, calorimetric, and size-based analysis approaches, including far-UV CD, fluorescence spectroscopy, DSC, SEC-MALS, single-particle mass photometry, and ATPase activity assays.

MATERIALS AND METHODS

Materials

Sodium chloride (catalog no. ASS270), imidazole (catalog no. ASI2835), SDS (catalog no. ASS2711), and acetic acid (catalog no. ASA1550) were purchased from Avra Synthesis (Hyderabad, India). Tryptone (cat #RM9111), yeast extract (cat #RM027), Coomassie brilliant blue R-250 (cat #MB153), ammonium persulfate (cat #MB003), TEMED (cat #MB026), acrylamide/bis acrylamide solution 40% (cat #ML083), and kanamycin acid sulfate (PCT1105) were purchased from Himedia (Mumbai, India). Tris (cat #79420), glycine (cat #64072), sodium phosphate dibasic dodecahydrate (cat #57085), isopropanol (cat #67800), agar powder (cat #19661), IPTG (cat #54110), PMSF (cat #87606), and DNAase (cat #14658) were purchased from SRL (Mumbai, India). Magnesium chloride hexahydrate (cat. no. DC0D693741), sodium dihydrogen phosphate monohydrate (cat. no. DF0D701140), 1,6-hexanediol (cat. no. H11807), thioflavin T (cat. no. T3516), and Amicon ultra centrifugal filter (30 kDa cutoff) (cat. no. UFC9030) were purchased from Merck. Qualigens hydrochloric acid (catalog no. Q29505), Qiagen Ni-NTA agarose (cat #30210) were used. Phosphate-buffered saline (PBS) buffer (catalog no. 1860454) was purchased from MP Biomedicals (Mumbai, India). All of the enzymes *Bam*HI-HF (cat. no. R3136S), *Hin*dIII-HF (cat. no. R2104S), T4DNA ligase (cat. no. M0202S), DpnI (cat. no. R0176S), T4 polynucleotide Kinase (cat.

https://doi.org/10.1021/acs.biochem.5c00642
Biochemistry XXXX, XXX, XXX−XXX

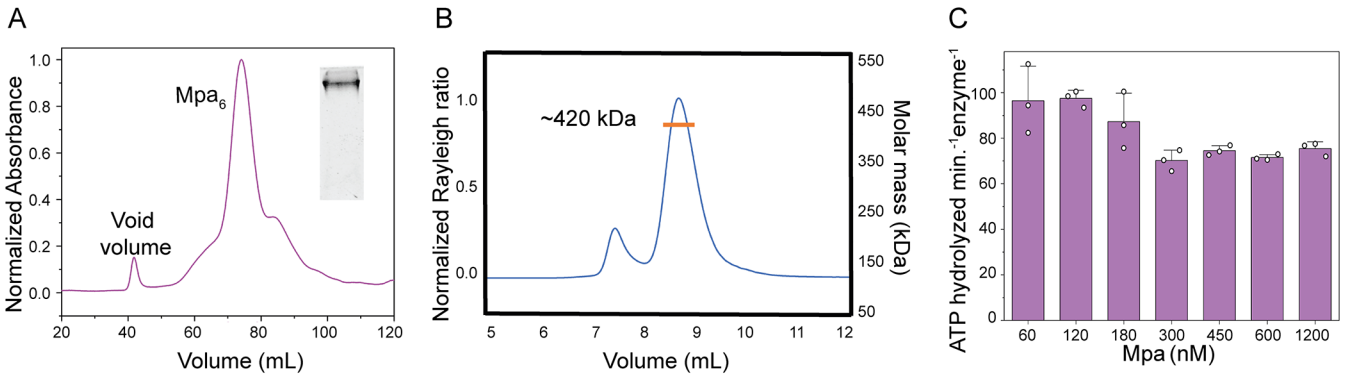

Figure 2. Size and ATPase activity analysis of Mpa: (A) Size exclusion chromatography showing a single major peak at ∼75 mL elution volume. Inset shows the native gel of the concentrated elutions from volumes 60 to 85 mL with a band corresponding to the size of a hexamer. (B) SEC-MALS analysis confirmed that the eluted peak corresponds to Mpa hexamer with a molecular mass of ∼420 kDa. (C) ATP hydrolysis rate as a function of Mpa monomer concentration showing no significant difference. Data are presented as the mean ± SD (n = 3). Individual data points are shown as white circles. Welch's t test was performed for the pair of two successive concentrations, and the difference is not significant with p > 0.05.

no. M0201S), and Q5 HF 2X Master mix (cat. no. M0492S) were purchased from NEB.

Methods

Protein Expression and Purification. Mycobacterial proteasomal activator (Mpa) gene (a gift from Heran Darwin's lab, NYU School of Medicine) was inserted into a modified plasmid vector pET-28a(+), with a hexahistidine tag and TEV restriction site at the N-terminus between the BamH1 and HindIII restriction sites. The plasmid containing the Mpa gene was transformed into *Escherichia coli* BL21DE3 competent cells, and the protein overexpression was induced at 37 °C by 0.5 mM IPTG for 4 h after OD_{600} reached 0.6. The bacterial cells were harvested at 4200 rpm for 20 min at 4 °C. Further, cells were resuspended in the lysis buffer (50 mM sodium phosphate, 200 mM NaCl, and 10% glycerol, pH 8) and lysed using a probe sonicator. The lysate was separated from cell debris by centrifugation and incubated with Ni-NTA beads at 4 °C. The beads were washed with wash buffer containing 10 mM imidazole and eluted using 300 mM imidazole. The eluents were concentrated and further purified by size exclusion chromatography (SEC) column using HiPrep 16/60 Sephacryl S-400 HR column and stored in SEC buffer (25 mM Tris.HCl, 200 mM NaCl, 10 mM $MgCl_2$, 1 mM DTT, 10% glycerol, pH 8).

Site-Directed Mutagenesis. Polymerase chain reaction (PCR) was performed on Mpa using suitable primers to obtain the gene encoding MpaW187F and MpaW570F. The PCR product was treated with a kinase, ligase, and DpnI (KLD) mixture and transformed into *E. coli* BL21DE3 competent cells. Plasmid was extracted from the colonies, and mutations were confirmed by Sanger sequencing.

Size Exclusion Chromatography-Multiangle Light Scattering (SEC-MALS). 3.6 mg/mL of Mpa_6 in SEC buffer was loaded onto a Superdex 200 10/300 column and separated at a flow rate of 0.3 mL/min. The molecular weight of the protein was calculated using Astra software.[27]

ATPase Activity Assay. ATP hydrolysis rate of Mpa was determined by NADH-coupled assay[28] on a multimode plate reader (Synergy H1M) at 37° C in SEC buffer by monitoring the decrease in NADH absorbance at 340 nm with time. For concentration-dependent studies, the Mpa monomer concentration was varied from 60 to 1200 nM, and for the mutant activity studies, 1200 nM Mpa was used. The assay and the ATP regeneration system components include 5 mM ATP, 0.4 mM NADH, 5 mM phosphoenolpyruvate, 20 U/mL pyruvate kinase, and 20 U/mL lactate dehydrogenase.

Nondenaturing (Native) PAGE Analysis. The Mpa samples were run on a 7.5% nondenaturing gel, visualized using a Bio-Rad Chemidoc imaging system, and image processing was done by ImageJ software. For studies at different salt concentrations, 1 μM Mpa_6 was incubated in SEC buffer with salt concentrations ranging from 0.15 to 3.2 M NaCl. For the chemical denaturation studies, 1 μM Mpa_6 was incubated in SEC buffer with urea concentrations ranging from 0 to 8 M at 25 °C for 16 h before loading onto the gel.

Far-UV Circular Dichroism spectroscopy. Chemical and thermal denaturation of Mpa_6 was analyzed by monitoring far-UV CD spectra in a Jasco J-815 spectropolarimeter. For chemical denaturation, the experiments were performed at 25 °C, whereas thermal denaturation was performed in the temperature range of 20 to 90 °C with 5 °C intervals at a temperature ramp rate of 2 °C/min.

Steady-State Fluorescence Experiments. For chemical unfolding studies, the tryptophan emission was monitored on a spectrofluorometer using an excitation wavelength of 295 nm, and the emission was recorded from 310 to 400 nm at 25 °C.

Single-Molecule Mass Photometry (MP) Studies. MP measurements were performed using a Refeyn Two MP instrument (Refeyn Ltd., U.K.) to determine the molecular mass and oligomeric states of the protein at different denaturant concentrations. All of the experiments were conducted at room temperature (25 °C). Denaturing mass photometry protocol as described by Gizardin-Fredon et al. was followed.[29] Briefly, a 100 nM Mpa_6 solution in PBS was incubated at different urea concentrations for 16 h at 25 °C, except for time-dependent and refolding studies. For each measurement, 18 μL of PBS buffer solution was placed on the silicon gasket, and the object was focused well through the "droplet dilution find focus" method. Next, 2 μL of the protein at different urea concentrations was added to this 18 μL buffer and mixed well, and the measurements were done immediately (final concentration is 10 nM Mpa_6). All of the acquisitions were recorded for 60 s in medium camera image view mode in the AcquireMP software. A contrast-to-mass calibration was conducted using Refeyn DiscoverMP software, using 20 nM BSA (66 kDa monomer and 132 kDa dimer) and thyroglobulin (660 kDa) proteins as standards. The maximum mass error of the calibration plot was 0.6%, and the R^2 value was 1.00.[29−31] A similar protocol was followed for time-dependent studies by varying the incubation time with 3 and 8 M urea and for refolding studies after removing the urea by dialysis.

Refolding Studies. To study the chemical refolding of Mpa, 1 μM Mpa_6 was incubated with 8 M urea (in SEC buffer) for 16 h at 25 °C. The refolding was performed by gradual removal of urea by dialysis, and the protein samples were collected at different urea concentrations during the refolding process. The samples were stored at 25 °C (except for fully refolded Mpa, which was stored at 4 °C).

Differential Scanning Calorimetry (DSC). Differential scanning calorimetry (DSC) experiments were performed in the tris buffer (25 mM Tris·HCl, 200 mM NaCl, 10 mM $MgCl_2$, 1 mM DTT, pH 8) using 5 μM Mpa_6 in a sample cell with a volume of 142 μL. Before loading into the calorimeter, the protein sample was thoroughly

https://doi.org/10.1021/acs.biochem.5c00642
Biochemistry XXXX, XXX, XXX−XXX

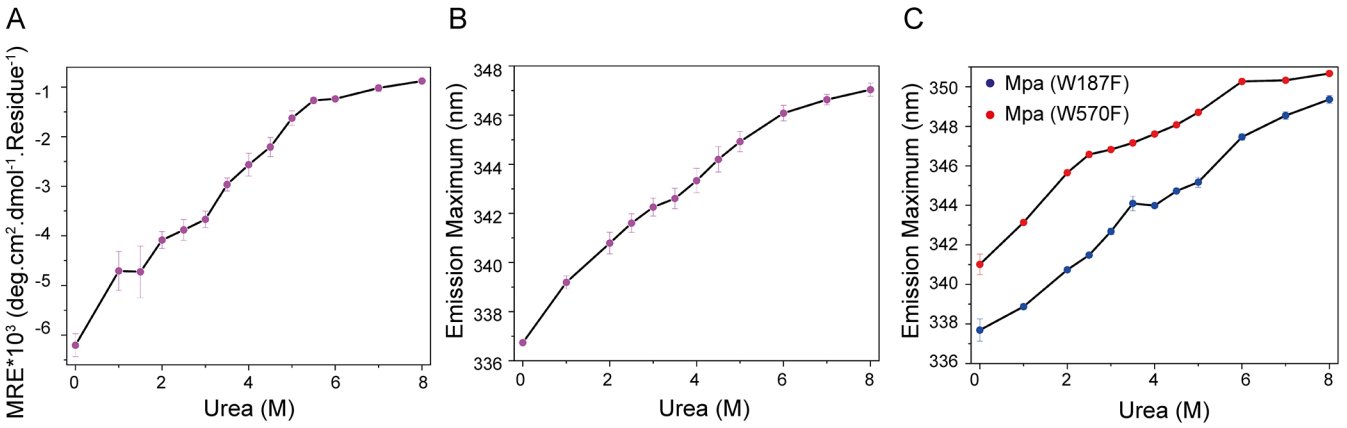

Figure 3. Chemical denaturation of Mpa_6: (A) Far-UV circular dichroism (CD) signal at 222 nm (MRE) of Mpa with increasing urea concentration, indicating a gradual loss of secondary structure. (B, C) Tryptophan fluorescence emission maxima (excited at 295 nm) of (B) wild-type Mpa and (C) its mutants, W187F and W570F, as a function of urea concentration. The blue and red circles represent the emission maximum for W187F and W570F mutants, respectively. Data are presented as the mean ± SD (n = 3).

desalted and degassed at 25 °C. The measurements were carried out on a MicroCal VP-Capillary automated DSC system (Malvern, U.K.), with temperature scans ranging from 5 to 95 °C at a ramp rate of 1 °C/min. Multiple buffer scans were recorded before each protein scan to assess and correct for thermal drift. During measurements, the calorimetric cells were pressurized to approximately 60 psi to minimize water evaporation at high temperatures.[32]

Nanodifferential Scanning Fluorimetry (Nano-DSF). Thermal denaturation of Mpa_6 was performed on a Prometheus Panta (NanoTemper) differential scanning fluorimetry (DSF) instrument, monitoring the tryptophan fluorescence. An excitation wavelength of 280 nm was used, and emission intensities were recorded at 330 and 350 nm. Measurements were performed over a temperature range of 20 to 90 °C, with a ramp rate of 1 °C/min. For refolding studies, samples were first heated from 20 to 50 °C/90 °C, followed by cooling from 50 °C/90 to 20 °C at the same scan rate. The ratio of fluorescence intensities (I_{350}/I_{330}) and its first derivative were analyzed to determine the melting temperature (T_m).[33]

Turbidity Assays. The temperature-dependent turbidity assay was conducted by measuring the optical density at 600 nm using a Jasco V-760 spectrophotometer. Measurements were taken over a temperature range of 20−90 °C with a ramp rate of 2 °C/min.

RESULTS

Size Analysis and ATPase Activity of Mpa_6

Size exclusion chromatography (SEC) analysis revealed that Mpa exists predominantly as a hexamer, even in the absence of any nucleotide, eluting as a single major peak (Figure 2A). Although a minor shoulder peak exists on both sides of the major peak, native polyacrylamide gel electrophoresis (PAGE) analysis showed that all of the elutions correspond to a single hexameric band (inset, Figure 2A). SEC coupled with multiangle light scattering (SEC-MALS) confirmed the size of the oligomeric state as 420 kDa, consistent with a hexameric assembly (Figure 2B). To determine the dependence of ATPase activity on the Mpa monomer concentration, which plausibly can suggest the presence of other oligomeric states,[34,35] ATPase rate was measured across a range of Mpa monomer concentrations. The enzyme exhibited a similar ATP hydrolysis rate of ∼80 ATPs/min/enzyme across all concentrations tested, including as low as 60 nM, suggesting a low dissociation constant and stable hexamer formation even at low monomer concentrations (Figures 2C and S2).

Urea-Induced Deoligomerization of Mpa_6

Chemical denaturation with urea was used to investigate the structural and oligomeric stabilities of Mpa_6. Native PAGE analysis revealed that a gradual disassembly of the hexamer directly to a monomeric species occurs, as observed by the appearance of a band corresponding to the size of the monomer with increasing urea concentration. Even at lower urea concentrations (0.5 M/1 M), a band corresponding to aggregated protein appears, which disappears as the urea concentration increases. Hexamers remained stable even up to 6 M urea, beyond which only a monomeric species remains, indicating the complete disassembly of hexamers (Figure S3). Far-UV circular dichroism (CD) spectra showed that the native protein exhibits minima at 222 and 208 nm, consistent with a predominantly α-helical structure (Figure S4). A gradual reduction in ellipticity at 222 nm was observed as the urea concentration increases, reflecting progressive loss of secondary structure, which continued until 5.5 M (Figures 3A and S4). To further assess changes in tertiary structure, tryptophan fluorescence emission spectra were recorded across the urea concentrations from 0 to 8 M. The emission maximum shifted gradually from 337 to 346 nm with increasing urea concentration (Figure 3B), indicating that tryptophan residues become more solvent-exposed. The emission maximum at 337 nm in the native state suggests that the tryptophans reside in a relatively polar environment.

Mpa contains two intrinsic tryptophan residues: W187, located in the OB2 domain, and W570, located within the ATPase domain. The changes observed in tryptophan fluorescence emission during chemical denaturation reflect an average response of both the residues. To resolve their individual contributions and confirm that the observed gradual increase is due to structural changes and not any averaging artifacts, we generated single tryptophan-to-phenylalanine mutants, Mpa(W187F) and Mpa(W570F), and analyzed their fluorescence properties independently. SEC profiles confirmed that both the mutants retained their native hexameric assembly (Figure S5A), and far-UV CD spectra (Figure S5B) showed no significant alterations in secondary structure relative to the wild-type protein. Fluorescence measurements revealed minor differences in the emission profiles of the two mutants. Mpa(W570F)′ which has the native W187 displayed a 3 nm red-shifted emission maximum

https://doi.org/10.1021/acs.biochem.5c00642
Biochemistry XXXX, XXX, XXX−XXX

relative to Mpa(W187F) (Figure S5C), consistent with a more solvent exposure around W187, supported by the SASA analysis. It also retains enzymatic activity, exhibiting an ATPase rate comparable to that of Mpa (WT). The W570 residue in Mpa is located near the ATP hydrolysis domain, and its mutation affected the activity, resulting in an approximately 30% reduction in ATPase rate (Figure S5D). Upon increasing urea concentration from 0 to 8 M, both the mutants exhibited a gradual red shift in emission maximum, increasing from 338 to 349 nm for Mpa(W187F) and 341 to 350 nm for Mpa(W570F) (Figure 3C). Both mutants exhibited similar denaturation patterns as observed for the wild-type protein. Together, CD and fluorescence data reveal a gradual, noncooperative denaturing mechanism. This could arise either from a stepwise disassembly of the oligomer (e.g., hexamer to trimer/dimer to monomer), followed by unfolding, or from a gradual shift of the equilibrium between hexameric and unfolded monomeric forms as the denaturant concentration increases. Native PAGE analysis shows a direct transition from the hexameric to the monomeric state without detectable intermediates, whereas spectroscopic data indicate a more gradual unfolding process.

Single-Particle Mass Photometry Analysis of Mpa

To resolve the ambiguity between the observations from native PAGE and spectroscopic analysis and further elucidate the mechanism of deoligomerization and denaturation, we employed single-particle mass photometry, a more sensitive technique capable of resolving intermediate oligomeric species based on mass and providing detailed insights into the disassembly pathway. Mass photometry measurements revealed that native Mpa predominantly exists as a hexamer (~420 kDa, ~96%), with a minor population of monomeric species (~70 kDa, 2.5%) that was not detected by SEC-MALS or native PAGE, underscoring the higher sensitivity of this technique (Figure 4A). These percentages represent the fraction of total Mpa molecules in hexameric and monomeric states rather than the stoichiometric ratio of hexamers to monomers. Upon gradual increase of the urea concentration, the hexamer population converted directly into monomeric species without significant accumulation of any other intermediate oligomeric species, and at 8 M urea, predominantly monomers were detected. A very minor population corresponding to a dimeric species was also observed in the native population; however, its proportion remained almost constant at all urea concentrations, including 8 M urea, making it unclear whether this peak reflects a genuine oligomeric species or a trace impurity. These results corroborate native PAGE analysis, confirming that Mpa exists primarily as a hexamer under native conditions and dissociates directly into monomeric species upon chemical destabilization. Complementing the overnight equilibrium studies, time-dependent analyses of 3 and 8 M urea–denatured Mpa_6 were performed to determine the presence of any other intermediate oligomeric species before the equilibrium is reached. We observed that the hexamer dissociates directly into monomeric species without significantly populating any intermediate oligomeric species, even at 1 min (Figures 4B and S6). These data reconfirm the concerted nature of hexamer disassembly. These monomeric species plausibly correspond to an unfolded state based on their red-shifted tryptophan fluorescence and loss of secondary structure.

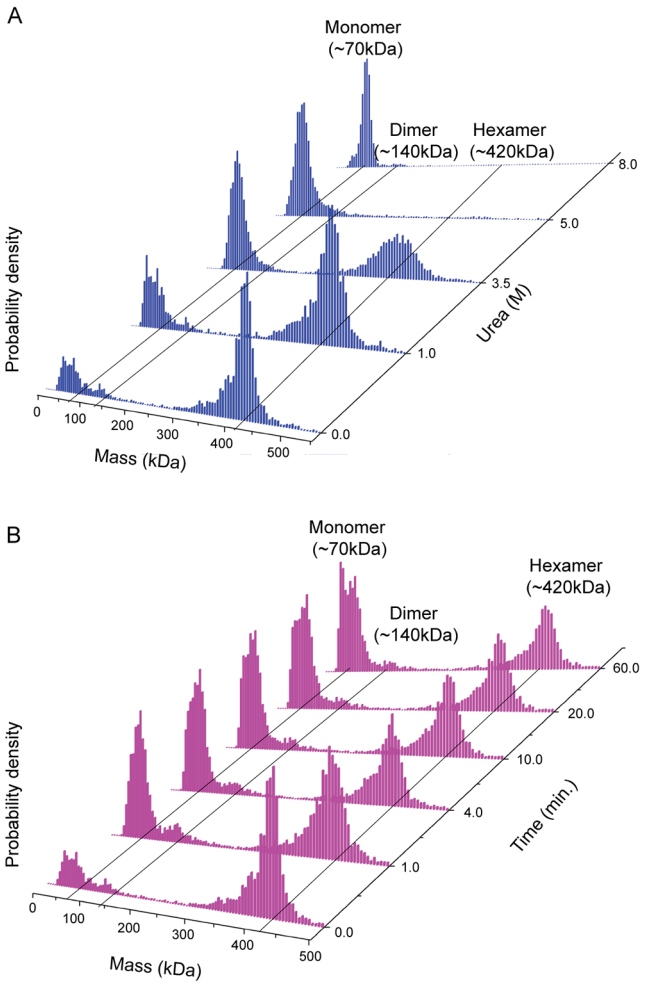

Figure 4. Mpa mass distributions analysis by single-particle mass photometry: (A) Mass distribution of Mpa in native form and at varying urea concentrations. (B) Variation in mass distribution with time for Mpa in 3 M urea.

Combining the size analysis and spectroscopic data results, it can be interpreted that the Mpa gradually transitions from a hexameric state to an unfolded monomeric state upon chemical denaturation, as observed by both native PAGE and mass photometry.

Probing the Stability of Mpa_6 by Perturbing the Electrostatic and Hydrophobic Interactions

To probe the contribution of electrostatic interactions to hexamer stability, Mpa was subjected to increasing salt concentrations ranging from 150 mM to 3.2 M NaCl, and the oligomeric state was analyzed by native PAGE and mass photometry. The hexameric assembly remained intact even at high salt concentrations (>2 M) (Figure S7A,B). Similarly, the Mpa_6 was also treated with 1,6-hexanediol to determine the effect of perturbing weak hydrophobic interactions among the monomers, and the hexameric state remains intact even at 5% (Figure S7C,D), indicating the stability of the hexamer and the role of both electrostatic and nonelectrostatic interactions in maintaining the oligomeric state. In both perturbations, higher concentrations of the additives cause the protein to aggregate at higher protein concentration (1 μM Mpa_6, native PAGE), whereas at lower protein concentration (10 nM Mpa_6, mass photometry), they lead to soluble monomeric species.

https://doi.org/10.1021/acs.biochem.5c00642
Biochemistry XXXX, XXX, XXX−XXX

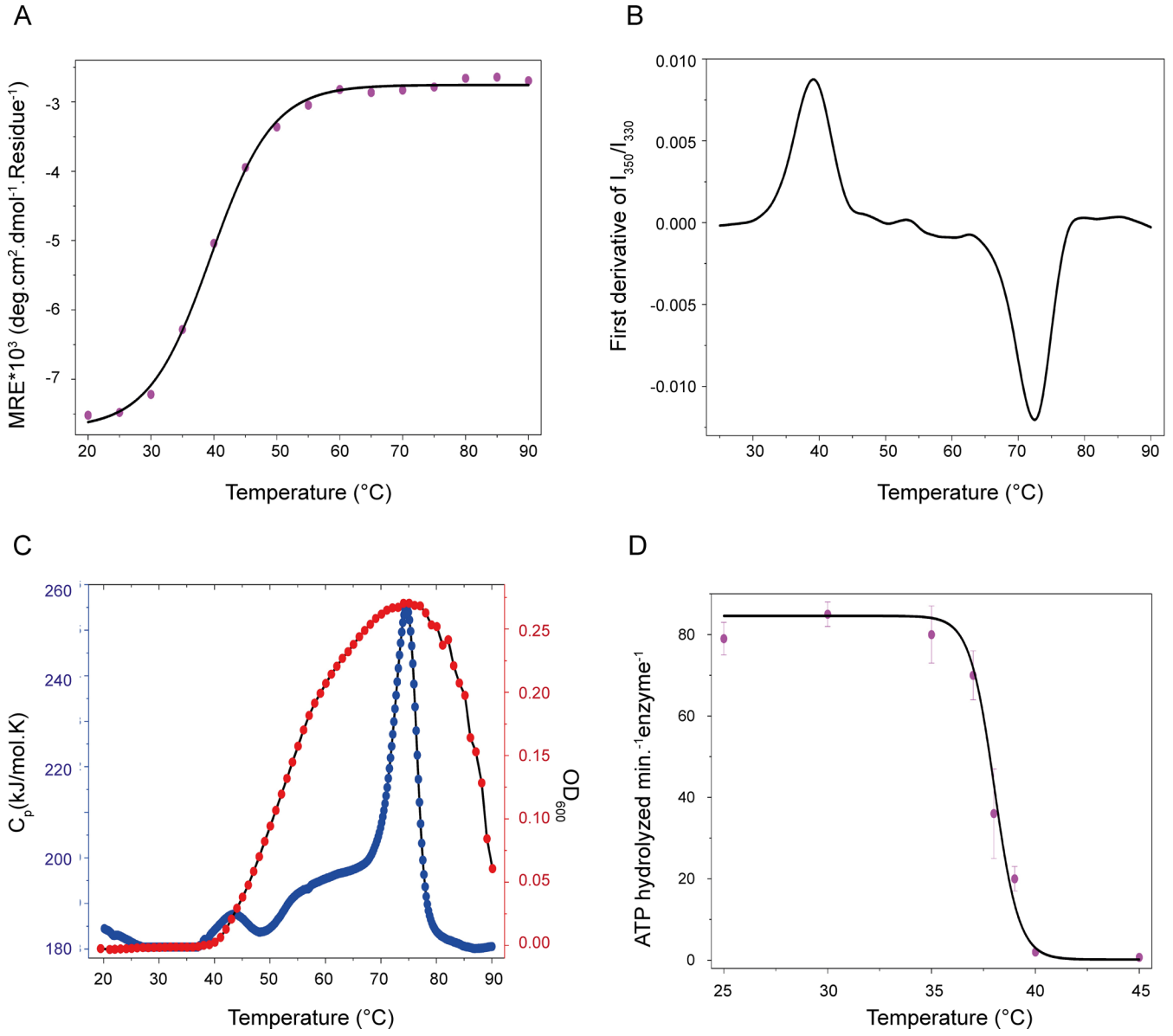

Figure 5. Thermal denaturation of Mpa_6: (A) Far-UV CD signal at 222 nm (MRE) of Mpa with increasing temperature, indicating a two-step denaturation process. The data was fitted to a sigmoidal curve. (B) First derivative of tryptophan fluorescence emission intensity ratio I_{350}/I_{330} (excited at 280 nm) with varying temperatures measured by nano-DSF, showing two transitions at 40 °C (positive derivative) and 73 °C (negative derivative). (C) Heat capacity plot (blue circles, left axis) from DSC with varying temperatures, showing two endothermic transitions at 45 and 75 °C. The turbidity plot (red circle; OD at 600 nm, right axis) shows an increase in turbidity at 40 °C, followed by a decrease in turbidity from 75 °C. (D) ATPase activity with increasing temperature. Above 37 °C, Mpa_6 ATPase activity drastically decreases, with complete loss at 40 °C. Data are presented as mean ± SD (n = 3). The data was fitted to a sigmoidal curve.

Temperature-Induced Deoligomerization of Mpa_6

Far-UV CD, nanodifferential scanning fluorimetry (nano-DSF), differential scanning calorimetry (DSC), turbidity, and activity assays were employed to investigate the deoligomerization pathway of Mpa under thermal perturbation. Unlike the gradual transitions observed during chemical denaturation, thermal unfolding monitored by the CD ellipticity at 222 nm displayed a cooperative transition with a midpoint at 40 °C (Figures 5A and S8). Tertiary structural changes assessed by nano-DSF, based on the first derivative of the I_{350}/I_{330} fluorescence ratio, revealed two distinct transitions at 40 and 73 °C (Figure 5B). DSC measurements detected two endothermic events: a lower amplitude peak at 45 °C and a higher amplitude peak at 75 °C (Figure 5C, left axis) in agreement with the nano-DSF results. To correlate structural changes with enzymatic function, the ATPase activity of Mpa was measured across a temperature gradient. Enzymatic activity declined sharply above 37 °C and was completely lost by 40 °C (Figure 5D), coinciding with the first transition peak detected by nano-DSF and DSC. Both the far-UV CD signal and enzymatic activity fitted well (R^2 > 0.98) to a sigmoidal curve, confirming a cooperative transition. Turbidity measurements at 600 nm further confirmed a steep increase in optical density above 40 °C, followed by a decline beyond 72 °C (Figure 5C, right axis). These transitions aligned well with the thermal unfolding profiles from DSC and nano-DSF. The initial rise in turbidity, followed by a decrease, likely reflects the formation of soluble aggregates that subsequently disaggregate

https://doi.org/10.1021/acs.biochem.5c00642
Biochemistry XXXX, XXX, XXX−XXX

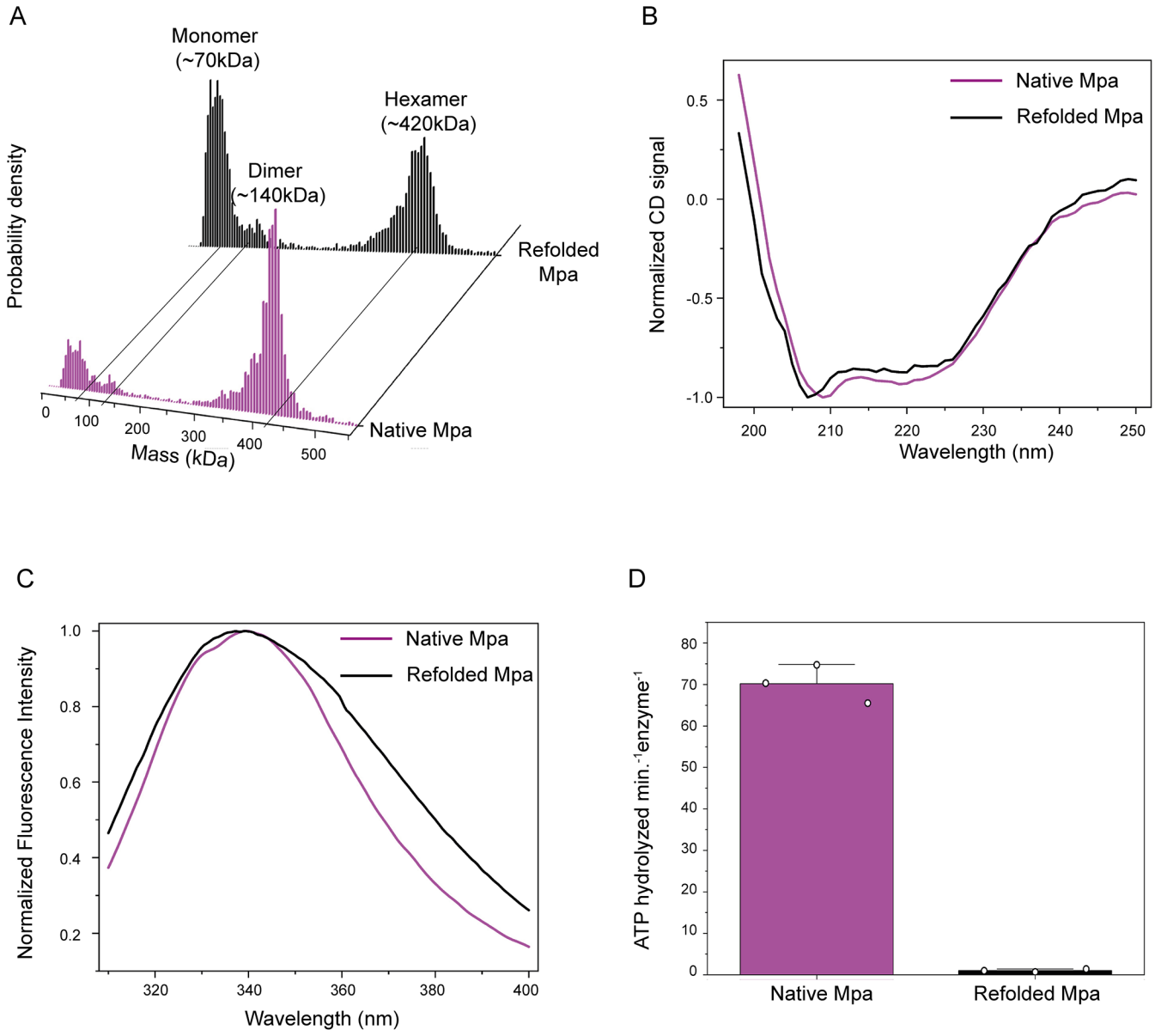

Figure 6. Refolding of chemically denatured Mpa: (A) Mass distributions, represented as a probability density, of native (purple) and refolded (black) Mpa measured by single-particle mass photometry. (B) Normalized far-UV CD spectra comparing native and refolded Mpa, indicating the gain of secondary structure upon refolding. (C) Normalized tryptophan fluorescence spectra (excitation at 295 nm) comparing native and refolded Mpa, indicating the gain of partial tertiary structure upon refolding. (D) ATPase activity of native and refolded Mpa, showing a loss of enzymatic activity upon refolding. Data are presented as mean ± SD (n = 3). Individual data points are shown in white circles.

into fully or partially unfolded monomers at higher temperatures. It is important to note that although a large fraction of protein remains in soluble form, a fraction of insoluble protein precipitates is also observed at temperatures >45 °C. The nature of the aggregates was probed by the thioflavin-T assay, which showed no change in the fluorescence intensity at higher temperatures, indicating nonamyloid aggregates[36] (Figure S9).

Refolding/Reoligomerization of Mpa after Chemical and Thermal Perturbation

To assess the structural and functional consequences of unfolding on refolding, native hexameric Mpa was chemically denatured in 8 M urea and subsequently refolded by reducing the urea concentration by slow dialysis. Native PAGE analysis during refolding revealed that a band corresponding to the size of the hexamer is observed only below ~1.5 M urea. Upon complete removal of the denaturant, unlike the native protein, the refolded protein did not fully reassemble into the hexameric state, and a substantial fraction remained in the monomeric form (Figure S10). The mass photometry analysis of the refolded protein shows that although a large fraction of the Mpa molecules corresponds to the mass of hexamers, the fraction of Mpa with the mass of monomers is higher than the native protein (Figure 6A). Far-UV CD spectra indicated that the refolded protein regained a secondary structure comparable to the native state (Figure 6B). Similarly, tryptophan fluorescence showed a blue shift in λ_{max} from 347 (unfolded) to 335 nm, approaching the native state. However, the broader emission spectrum suggested that the refolded protein adapted a compact, native-like conformation rather than a fully native structure (Figure 6C). Functionally, the refolded protein exhibited a complete loss of ATPase activity (Figure 6D).

https://doi.org/10.1021/acs.biochem.5c00642
Biochemistry XXXX, XXX, XXX−XXX

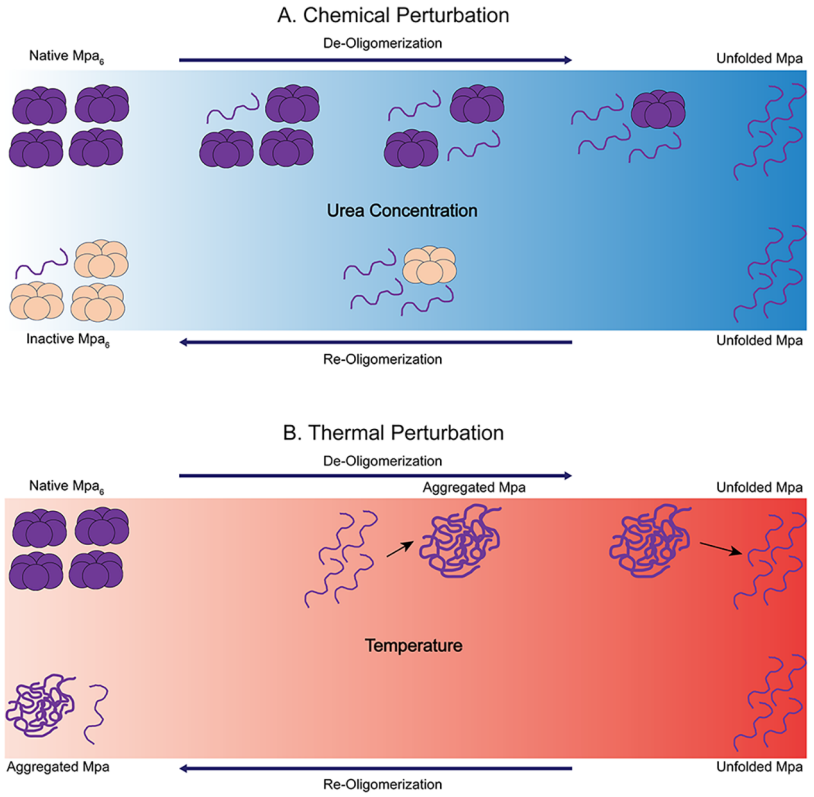

Figure 7. Proposed model for Mpa deoligomerization by chemical (A) and thermal (B) perturbation: (A) Chemical perturbation: Upon urea treatment, Mpa_6 deoligomerizes in a concerted but noncooperative manner, directly converting into a soluble, unfolded monomer gradually without any detectable intermediate. Upon refolding, it predominantly forms enzymatically inactive hexamers, and a minor population exists as monomers. The blue gradient indicates an increase in the urea concentration. (B) Thermal perturbation: Upon thermal stress, Mpa_6 deoligomerizes in both a concerted and cooperative manner. It initially unfolds and spontaneously forms nonamyloid-like aggregates; further heating results in a soluble, unfolded structure. Thermal unfolding of Mpa_6 is irreversible. The red gradient indicates an increase in the temperature.

Consistent with this, thermal unfolding was irreversible: heating to either 50 or 90 °C resulted in permanent loss of enzymatic activity with no recovery upon cooling (Figure S11).

DISCUSSION

Mpa is an AAA+ enzyme that complexes with 20S CP in *M. tuberculosis* and catalyzes substrate protein unfolding and translocation prior to its degradation.[37−39] In this study, we investigated the stability, activity, and mechanisms of deoligomerization and reoligomerization of this homohexameric enzyme using chemical and thermal perturbants. Mpa assembles into stable hexamers even at submicromolar concentrations, indicative of a strong intrinsic self-association affinity. ATPase activity measurements and mass photometry confirmed that, in the presence and absence of ATP, respectively, Mpa remains in a hexameric form even at tens of nanomolar concentrations. Although structural studies suggest that individual monomers are primarily stabilized by electrostatic interactions,[23] the hexamer persists even at very high salt concentrations and 1,6-hexanediol, indicating the role of both electrostatic and nonelectrostatic interactions in maintaining its stability.

During chemical denaturation, far-UV CD and tryptophan fluorescence analyses revealed gradual changes in ellipticity and emission maxima, respectively, with increasing urea concentrations. This gradual increase suggests either a multistep denaturation process involving other oligomeric states as the protein transitions from the hexamer to the unfolded state or a gradual conversion of hexamers to unfolded monomers, noncooperatively. Native PAGE analyses showed that Mpa dissociates directly from the hexameric to monomeric species without detectable intermediates as the urea concentration increases. Single-particle mass photometry resolved this discrepancy, showing that the transition is concerted, where the hexamer directly deoligomerizes to monomeric species even at low urea concentrations, with the monomer population progressively increasing as urea concentration rises. Recently, a similar result was observed using mass photometry on ADH and GLDH homo-oligomers that transition directly to the monomeric species without significantly populating other oligomeric states upon chemical denaturation.[29] Thus, the continuous changes observed during CD and fluorescence measurements in our studies reflect a shifting equilibrium between hexamers and monomers rather than the accumulation of intermediate oligomeric states. Furthermore, the red shift in tryptophan fluorescence and the reduction in ellipticity at 222 nm upon increasing the denaturant concentration indicate that the monomeric species populated is unfolded. These findings suggest that Mpa undergoes a transition from the hexameric state to an unfolded monomer. These transitions are noncooperative, where the deoligomerization between the subunits is not strongly coupled, and each subunit deoligomerizes independently, hence the gradual change in the spectroscopic signatures. The refolding of chemically perturbed Mpa is not completely reversible. Upon refolding, Mpa regains its secondary structure and a globular conformation; however, the extent of

https://doi.org/10.1021/acs.biochem.5c00642
Biochemistry XXXX, XXX, XXX−XXX

hexamerization in the refolded sample is significantly reduced compared with the native protein, and the refolded enzyme is catalytically inactive. This is in contrast to some of the other AAA+ enzymes such as p97 that regain both oligomeric state and catalytic activity upon refolding.[16] Hence, Mpa undergoes a concerted but noncooperative deoligomerization upon perturbation by urea, and the reoligomerization results in an inactive assembly (Figure 7A).

The thermal denaturation of Mpa hexamers follows a path slightly different from the chemical denaturation. The deoligomerization is both concerted and cooperative. The hexamers are unstable at temperatures as low as 40 °C and lose their catalytic activity beyond this temperature. Nano-DSF, DSC, and turbidity measurements consistently reveal two distinct transitions at ∼40 °C and ∼70 °C. The first transition corresponds to unfolding of the Mpa as evident from the decrease in the ellipticity at 222 nm of the *f*ar-UV CD spectrum and a red-shifted tryptophan fluorescence maximum. Incidentally, the turbidity measurements show a sudden increase in the optical density at this temperature, indicating the further aggregation of the protein. These results taken together implicate that initially unfolding occurs, which is an endothermic event, followed by spontaneous aggregation, which is an exothermic event. Overall, a minor positive peak during DSC implies that the heat changes during the unfolding substantially negate the heat changes during aggregation, resulting in a low magnitude endothermic transition at this temperature. Overall, it can be concluded that at 40 °C, the Mpa undergoes unfolding followed by spontaneous aggregation. Interestingly, this temperature overlaps with the loss of ATPase activity, concluding that ATP does not increase the thermal stability, as both the apo form (from *the* turbidity assay) and nucleotide-bound form (from *the* ATPase assay) show transitions at the same temperature. Second transition: a higher magnitude endothermic event in DSC, a negative peak in nano-DSF, and a decrease in turbidity were observed at ∼70 °C. These results implicate that at this higher temperature, the disaggregation of the aggregates occurs, plausibly into majorly unfolded monomers. Overall, upon thermal perturbation, Mpa unfolds and spontaneously aggregates. Further heating results in the disaggregation and unfolding of Mpa. In addition, a fraction of the aggregates precipitates out as the temperature increases. The thermal denaturation is completely irreversible with respect to oligomerization, unlike chemical denaturation, which showed partial hexamerization (Figure 7B). Based on both chemical and thermal deoligomerization analyses, it can be concluded that Mpa forms obligate oligomers that unfold upon perturbation[40,41] These unfolded monomers tend to aggregate, which can be seen during the thermal denaturation. During the chemical denaturation, the aggregation of these unfolded monomers was observed at lower urea concentration, but it is plausibly prevented at higher urea concentrations, which is known to act as a stabilizing agent against aggregation.[42]

CONCLUSIONS

Our studies on the effects of chemical and thermal perturbants on the oligomeric assembly of Mpa demonstrate that its disassembly proceeds through a concerted rather than stepwise mechanism. Notably, the exact pathways differ depending on the perturbant: chemical denaturation drives a concerted but noncooperative process, whereas thermal perturbation induces a concerted and cooperative transition. The unfolded proteins fail to refold reversibly, instead leading to inactive complexes. While many homo-oligomeric proteins are known to dissociate through stepwise mechanisms, our findings provide an example of a homooligomer undergoing a concerted disassembly. These observations raise intriguing questions about the evolutionary and structural factors that dictate the choice between concerted and stepwise oligomerization/deoligomerization pathways. Future investigations combining mutational studies, single-particle mass photometry, with complementary ensemble biophysical approaches on other AAA+ systems could help identify the molecular interactions that govern concerted or stepwise deoligomerization pathways of these enzymes.

ASSOCIATED CONTENT

Supporting Information

The Supporting Information is available free of charge at https://pubs.acs.org/doi/10.1021/acs.biochem.5c00642.

Spontaneous formation of homohexamers Mpa (Figure S1); ATPase activity of Mpa (Figure S2); stability of Mpa hexamer with varying urea concentrations (Figure S3); Far-UV CD spectra of Mpa with varying urea concentrations (Figure S4); size and structural comparison of Mpa and its mutants (Figure S5); variation in mass distribution with time for Mpa in 8 M urea measured by single-particle mass photometry (Figure S6); stability of Mpa hexamer with varying NaCl and 1,6-hexanediol concentrations (Figure S7); Far-UV CD spectra of Mpa with varying temperatures (Figure S8); thioflavin T (ThT) binding assay for Mpa aggregates (Figure S9); refolding analysis of chemically denatured Mpa (Figure S10); refolding analysis of thermally denatured Mpa (Figure S11) (PDF)

Accession Codes

Protein (UniProt ID): Mpa (P9WQN4)

AUTHOR INFORMATION

Corresponding Author

Hema Chandra Kotamarthi − *Department of Chemistry, Indian Institute of Technology Madras, Chennai 600036, India*; orcid.org/0000-0003-0278-1376; Email: hemachandra@iitm.ac.in

Authors

Pushpkant Sahu − *Department of Chemistry, Indian Institute of Technology Madras, Chennai 600036, India*

Samapti Mondal − *Department of Chemistry, Indian Institute of Technology Madras, Chennai 600036, India*

Bincy Lukose − *Department of Biotechnology, Indian Institute of Technology Madras, Chennai 600036, India*

Thalappil Pradeep − *Department of Chemistry, Indian Institute of Technology Madras, Chennai 600036, India; International Centre for Clean Water, IIT Madras Research Park, Chennai 600113, India*; orcid.org/0000-0003-3174-534X

Complete contact information is available at: https://pubs.acs.org/10.1021/acs.biochem.5c00642

Author Contributions

H.C.K. conceived the study, supervised the project, and acquired the funding. H.C.K. and P.K.S. designed the experiments. P.K.S. performed the experiments, analyzed the

https://doi.org/10.1021/acs.biochem.5c00642
Biochemistry XXXX, XXX, XXX−XXX

data, and prepared the figures. H.C.K. and P.K.S. wrote the manuscript. S.M. performed, and S.M. and T.P. analyzed the mass photometry experiments. B.L. performed DSC experiments. All of the authors contributed to the revision of the manuscript.

Notes

The authors declare no competing financial interest.

■ ACKNOWLEDGMENTS

H.C.K. thanks the Department of Biotechnology, India, for the Grant BT/PR44858/MED/29/1608/2022, DST-FIST, and the Department of Chemistry and Department of Biotechnology, IIT Madras, for the infrastructure facilities. P.K.S. thanks the Government of India for the PMRF fellowship. We thank Prof. Athi Naganathan, Department of Biotechnology, for the DSC facility; Dr. Radha Chauhan, NCCS Pune, for the SEC-MALS; and Mr. Sindhura and his team from NanoTemper for the nano-DSF measurements.

■ REFERENCES

(1) Hashimoto, K.; Nishi, H.; Bryant, S.; Panchenko, A. R. Caught in Self-Interaction: Evolutionary and Functional Mechanisms of Protein Homooligomerization. *Phys. Biol.* **2011**, *8* (3), No. 035007.
(2) Goodsell, D. S.; Olson, A. J. Structural Symmetry and Protein Function. *Annu. Rev. Biophys. Biomol. Struct.* **2000**, *29* (1), 105−153.
(3) Ali, M. H.; Imperiali, B. Protein Oligomerization: How and Why. *Bioorg. Med. Chem.* **2005**, *13* (17), 5013−5020.
(4) Cornish-Bowden, A. J.; Koshland, D. E. The Quaternary Structure of Proteins Composed of Identical Subunits. *J. Biol. Chem.* **1971**, *246* (10), 3092−3102.
(5) Baisamy, L.; Jurisch, N.; Diviani, D. Leucine Zipper-Mediated Homo-Oligomerization Regulates the Rho-GEF Activity of AKAP-Lbc. *J. Biol. Chem.* **2005**, *280* (15), 15405−15412.
(6) Abulimiti, A.; Fu, X.; Gu, L.; Feng, X.; Chang, Z. Mycobacterium Tuberculosis Hsp16.3 Nonamers Are Assembled and Re-Assembled via Trimer and Hexamer Intermediates. *J. Mol. Biol.* **2003**, *326* (4), 1013−1023.
(7) Feng, Y.; Jiao, W.; Fu, X.; Chang, Z. Stepwise Disassembly and Apparent Nonstepwise Reassembly for the Oligomeric RbsD Protein. *Protein Sci.* **2006**, *15* (6), 1441−1448.
(8) Sauer, R. T.; Baker, T. A. AAA+ Proteases: ATP-Fueled Machines of Protein Destruction. *Annu. Rev. Biochem.* **2011**, *80* (1), 587−612.
(9) Yedidi, R. S.; Wendler, P.; Enenkel, C. AAA-ATPases in Protein Degradation. *Front. Mol. Biosci.* **2017**, *4*, No. 42, DOI: 10.3389/fmolb.2017.00042.
(10) Butler, S. M.; Festa, R. A.; Pearce, M. J.; Darwin, K. H. Self-compartmentalized Bacterial Proteases and Pathogenesis. *Mol. Microbiol.* **2006**, *60* (3), 553−562.
(11) Duderstadt, K. E.; Berger, J. M. AAA+ ATPases in the Initiation of DNA Replication. *Crit. Rev. Biochem. Mol. Biol.* **2008**, *43* (3), 163−187.
(12) Beyer, A. Sequence Analysis of the AAA Protein Family. *Protein Sci.* **1997**, *6* (10), 2043−2058.
(13) Veronese, P. K.; Rajendar, B.; Lucius, A. L. Activity of *E. Coli* ClpA Bound by Nucleoside Diphosphates and Triphosphates. *J. Mol. Biol.* **2011**, *409* (3), 333−347.
(14) Hersch, G. L.; Burton, R. E.; Bolon, D. N.; Baker, T. A.; Sauer, R. T. Asymmetric Interactions of ATP with the AAA+ ClpX6 Unfoldase: Allosteric Control of a Protein Machine. *Cell* **2005**, *121* (7), 1017−1027.
(15) Veronese, P. K.; Lucius, A. L. Effect of Temperature on the Self-Assembly of the *Escherichia Coli* ClpA Molecular Chaperone. *Biochemistry* **2010**, *49* (45), 9820−9829.
(16) Wang, Q.; Song, C.; Li, C.-C. H. Hexamerization of P97-VCP Is Promoted by ATP Binding to the D1 Domain and Required for ATPase and Biological Activities. *Biochem. Biophys. Res. Commun.* **2003**, *300* (2), 253−260.
(17) Baker, T. A.; Sauer, R. T. ATP-Dependent Proteases of Bacteria: Recognition Logic and Operating Principles. *Trends Biochem. Sci.* **2006**, *31* (12), 647−653.
(18) Djuranovic, S.; Hartmann, M. D.; Habeck, M.; Ursinus, A.; Zwickl, P.; Martin, J.; Lupas, A. N.; Zeth, K. Structure and Activity of the N-Terminal Substrate Recognition Domains in Proteasomal ATPases. *Mol. Cell* **2009**, *34* (5), 580−590.
(19) Wang, Q.; Song, C.; Yang, X.; Li, C.-C. H. D1 Ring Is Stable and Nucleotide-Independent, Whereas D2 Ring Undergoes Major Conformational Changes during the ATPase Cycle of P97-VCP. *J. Biol. Chem.* **2003**, *278* (35), 32784−32793.
(20) Yin, Y.; Kovach, A.; Hsu, H.-C.; Darwin, K. H.; Li, H. The Mycobacterial Proteasomal ATPase Mpa Forms a Gapped Ring to Engage the 20S Proteasome. *J. Biol. Chem.* **2021**, *296*, No. 100713.
(21) Thomas, A. A.; Dougan, D. A. AAA+ Machines of Protein Destruction in Mycobacteria. *Front Mol. Biosci.* **2017**, *4*, No. 49, DOI: 10.3389/fmolb.2017.00049.
(22) Kavalchuk, M.; Jomaa, A.; Müller, A. U.; Weber-Ban, E. Structural Basis of Prokaryotic Ubiquitin-like Protein Engagement and Translocation by the Mycobacterial Mpa-Proteasome Complex. *Nat. Commun.* **2022**, *13* (1), No. 276.
(23) Wang, T.; Li, H.; Lin, G.; Tang, C.; Li, D.; Nathan, C.; Darwin, K. H.; Li, H. Structural Insights on the Mycobacterium Tuberculosis Proteasomal ATPase Mpa. *Structure* **2009**, *17* (10), 1377−1385.
(24) Djuranovic, S.; Hartmann, M. D.; Habeck, M.; Ursinus, A.; Zwickl, P.; Martin, J.; Lupas, A. N.; Zeth, K. Structure and Activity of the N-Terminal Substrate Recognition Domains in Proteasomal ATPases. *Mol. Cell* **2009**, *34* (5), 580−590.
(25) Levy, E. D.; Erba, E. B.; Robinson, C. V.; Teichmann, S. A. Assembly Reflects Evolution of Protein Complexes. *Nature* **2008**, *453* (7199), 1262−1265.
(26) Levy, E. D.; Pereira-Leal, J. B.; Chothia, C.; Teichmann, S. A. 3D Complex: A Structural Classification of Protein Complexes. *PLoS Comput. Biol.* **2006**, *2* (11), No. e155.
(27) Some, D.; Amartely, H.; Tsadok, A.; Lebendiker, M. Characterization of Proteins by Size-Exclusion Chromatography Coupled to Multi-Angle Light Scattering (SEC-MALS). *J. Visualized Exp.* **2019**, *148*, No. e59615.
(28) Kotamarthi, H. C.; Sauer, R. T.; Baker, T. A. The Non-Dominant AAA+ Ring in the ClpAP Protease Functions as an Anti-Stalling Motor to Accelerate Protein Unfolding and Translocation. *Cell Rep.* **2020**, *30* (8), 2644−2654.e3.
(29) Gizardin-Fredon, H.; Santo, P. E.; Chagot, M.-E.; Charpentier, B.; Bandeiras, T. M.; Manival, X.; Hernandez-Alba, O.; Cianférani, S. Denaturing Mass Photometry for Rapid Optimization of Chemical Protein-Protein Cross-Linking Reactions. *Nat. Commun.* **2024**, *15* (1), No. 3516.
(30) Roy, J.; Marathe, I.; Wysocki, V.; Pradeep, T. Observing Atomically Precise Nanocluster Aggregates in Solution by Mass Photometry. *Chem. Commun.* **2024**, *60* (52), 6655−6658.
(31) Asor, R.; Kukura, P. Characterising Biomolecular Interactions and Dynamics with Mass Photometry. *Curr. Opin. Chem. Biol.* **2022**, *68*, No. 102132.
(32) Lukose, B.; Maruno, T.; Faidh, M. A.; Uchiyama, S.; Naganathan, A. N. Molecular and Thermodynamic Determinants of Self-Assembly and Hetero-Oligomerization in the Enterobacterial Thermo-Osmo-Regulatory Protein H-NS. *Nucleic Acids Res.* **2024**, *52* (5), 2157−2173.
(33) Chattopadhyay, G.; Varadarajan, R. Facile Measurement of Protein Stability and Folding Kinetics Using a Nano Differential Scanning Fluorimeter. *Protein Sci.* **2019**, *28* (6), 1127−1134.
(34) Singh, J.; Anand, R.; Horovitz, A. Cooperativity in ATP Hydrolysis by MopR Is Modulated by Its Signal Reception Domain and by Its Protein and Phenol Concentrations. *J. Bacteriol.* **2022**, *204* (8), No. e0017922, DOI: 10.1128/jb.00179-22.
(35) Vieux, E. F.; Wohlever, M. L.; Chen, J. Z.; Sauer, R. T.; Baker, T. A. Distinct Quaternary Structures of the AAA+ Lon Protease

Control Substrate Degradation. *Proc. Natl. Acad. Sci. U.S.A.* **2013**, *110* (22), E2002−E2008, DOI: 10.1073/pnas.1307066110.
(36) Biancalana, M.; Koide, S. Molecular Mechanism of Thioflavin-T Binding to Amyloid Fibrils. *Biochim. Biophys. Acta, Proteins Proteomics* **2010**, *1804* (7), 1405−1412.
(37) Striebel, F.; Hunkeler, M.; Summer, H.; Weber-Ban, E. The Mycobacterial Mpa−Proteasome Unfolds and Degrades Pupylated Substrates by Engaging Pup's N-Terminus. *EMBO J.* **2010**, *29* (7), 1262−1271.
(38) Kavalchuk, M.; Jomaa, A.; Müller, A. U.; Weber-Ban, E. Structural Basis of Prokaryotic Ubiquitin-like Protein Engagement and Translocation by the Mycobacterial Mpa-Proteasome Complex. *Nat. Commun.* **2022**, *13* (1), No. 276.
(39) Darwin, K. H.; Lin, G.; Chen, Z.; Li, H.; Nathan, C. F. Characterization of a *Mycobacterium Tuberculosis* Proteasomal ATPase Homologue. *Mol. Microbiol.* **2005**, *55* (2), 561−571.
(40) Mintseris, J.; Weng, Z. Structure, Function, and Evolution of Transient and Obligate Protein−Protein Interactions. *Proc. Natl. Acad. Sci. U.S.A.* **2005**, *102* (31), 10930−10935.
(41) Nooren, I. M. A. NEW EMBO MEMBER'S REVIEW: Diversity of Protein-Protein Interactions. *EMBO J.* **2003**, *22* (14), 3486−3492.
(42) Remmele, R. L.; Enk, J. Z.-v.; Phan, D.; Yu, L. Stabilization by Urea during Thermal Unfolding-Mediated Aggregation of Recombinant Human Interleukin-1 Receptor (Type II): Does Solvation Entropy Play a Role? *J. Phys. Chem. B* **2012**, *116* (24), 7240−7251.

https://doi.org/10.1021/acs.biochem.5c00642
Biochemistry XXXX, XXX, XXX−XXX